

Morphological/SAXS/WAXS studies on the electrochemical synthesis of graphene nanoplatelets



S.N. Hosseini Abbandanak^a, H. Aghamohammadi^a, E. Akbarzadeh^{a,*}, N. Shabani^b,
R. Eslami-Farsani^a, M. Kangooie^b, M. Hossein Siadati^a

^a Faculty of Materials Science and Engineering, K. N. Toosi University of Technology, Tehran, Iran

^b Armina Engineering Company, Pardis Technology Park, Tehran, Iran

ARTICLE INFO

Keywords:

Electrochemical exfoliation
Graphite
Graphene
SAXS
WAXS
Morphology

ABSTRACT

Recently, graphene owing to its outstanding properties such as high mechanical strength, high thermal and electrical conductivity has been introduced as a surprising material for various applications. Up to now, the introduced methods mostly have some disadvantageous, especially in term of efficiency. Electrochemical exfoliation of graphite is a cost-effective, fast and environmentally friendly method for the synthesis of graphene nanoplatelets (GNPs). Based on this fact that the properties of GNPs are greatly depend on their morphology, the aim of this study was to evaluate the morphology of the obtained powders after electrochemical exfoliation of graphite by scanning electron microscopy. In this work, the mixture of $H_2SO_4 + NaOH + H_2O_2$ was used as the electrolyte. Effects of three concentrations of H_2SO_4 on the morphology of the obtained powders was examined. After determining the optimum sample, the analyses of transmission electron microscopy, X-ray diffraction, Raman spectroscopy and FTIR were used to characterize the produced GNPs by this method. Further characterization on the optimized sample was carried out by synchrotron small and wide angle X-ray scattering (SAXS/WAXS) to understand the shape and fractality of particles which have been confirmed to the initial results. Results indicated that based on electrolyte type and concentration of H_2SO_4 , different kinds of carbon allotropes such as expanded graphite, multi-layered GNPs and few-layered GNPs can be obtained. Results showed the efficiency of the electrochemical method was increased with decreasing the concentration of the H_2SO_4 ; the few-layered GNPs were obtained using the lowest concentration of H_2SO_4 .

1. Introduction

Graphene, a two-dimensional material, is a single layer of carbon atoms arrayed in a hexagonal pattern comprised of sp^2 hybridized bonding. Due to its outstanding mechanical, electrical, thermal and optical properties, graphene has attracted great attention in the scientific and industrial societies. Outstanding mechanical properties of graphene sheets can be attributed to the very strong bonding between carbon atoms while its thermal and electrical properties are due to the sp^2 hybridization [1–4]. To date, different methods including bottom-up (e.g., chemical vapor deposition) and top-down approaches (e.g., laser ablation) have been introduced for the synthesis of graphene nanoplatelets (GNPs). However, these methods generally have various disadvantageous such as inappropriate for large-scale production, high cost of production, obtaining multi-layered GNPs, structural defects, etc. [4–9].

Electrochemical exfoliation of graphite is one of the introduced

approaches in recent years for the synthesis of GNPs. It has been reported that the high quality and few-layered GNPs can be obtained using electrochemical exfoliation of graphite. Simplicity and ability to large-scale production of GNPs are the main advantages of this method. In spite of these advantages, it is worth noting that the efficiency of this approach greatly depends on several parameters such as electrodes, electrolytes and electrochemistry conditions. Generally, electrochemical synthesis of GNPs can be done through anodic exfoliation or cathodic exfoliation. From performed studies, it has been well-understood that the quality of the obtained GNPs by anodic exfoliation is higher than that of prepared GNPs by cathodic exfoliation [10–17]. Up to now, different electrolytes such as sulfuric acid, nitric acid and phosphoric acid have been used for anodic exfoliation of graphite by various investigations. In these studies, it is well-established that the efficiency of electrolytes containing sulfate ions is higher than that of other used electrolytes. For example, Parvez et al. [14] investigated the effects of different electrolytes including $(NH_4)_2SO_4$, Na_2SO_4 , K_2SO_4 ,

* Corresponding author.

E-mail address: a3brahim@gmail.com (E. Akbarzadeh).

<https://doi.org/10.1016/j.ceramint.2019.07.077>

Received 31 May 2019; Received in revised form 6 July 2019; Accepted 7 July 2019

Available online 08 July 2019

0272-8842/ © 2019 Elsevier Ltd and Techna Group S.r.l. All rights reserved.

Table 1
The code of HF treated powders.

Sample	Code
Pristine graphite electrode	PG
Exfoliated graphite in 1.6 M H ₂ SO ₄	EG1
Exfoliated graphite in 1.6 M H ₂ SO ₄ + 0.03 M NaOH + 0.5 M H ₂ O ₂	EG2
Exfoliated graphite in 1.2 M H ₂ SO ₄ + 0.03 M NaOH + 0.5 M H ₂ O ₂	EG3
Exfoliated graphite in 0.6 M H ₂ SO ₄ + 0.03 M NaOH + 0.5 M H ₂ O ₂	EG4

NH₄Cl, NaNO₃ and NaClO₄ and their results indicated that the efficiency of sulfate ion electrolytes was the highest in the production of high-quality GNPs.

As far as we know, previous works only have focused on the effects of electrolyte type on the electrochemical exfoliation of graphite and the impacts of electrolyte concentration on the efficiency of this method have not been dealt with in depth. Therefore, the main aim of this work is to investigate the effect of electrolyte on the efficiency of electrochemical exfoliation of graphite. In this work, attempts were made to exfoliate pristine graphite (PG) to form exfoliated graphite (EG) and ultimately GNPs. First, the effect of sulfuric acid electrolyte concentration on the morphology of obtained EG samples was evaluated by scanning electron microscopy (SEM) images and X-ray diffraction (XRD) analyses. Then, after characterization of optimal sample, further analyses including transmission electron microscopy (TEM), Raman spectroscopy, Fourier transformation infrared (FTIR), small and wide angle X-ray scattering (SAXS/WAXS) have been carried out to distinguish the shape, fractal nature and crystalline structure of the GNPs.

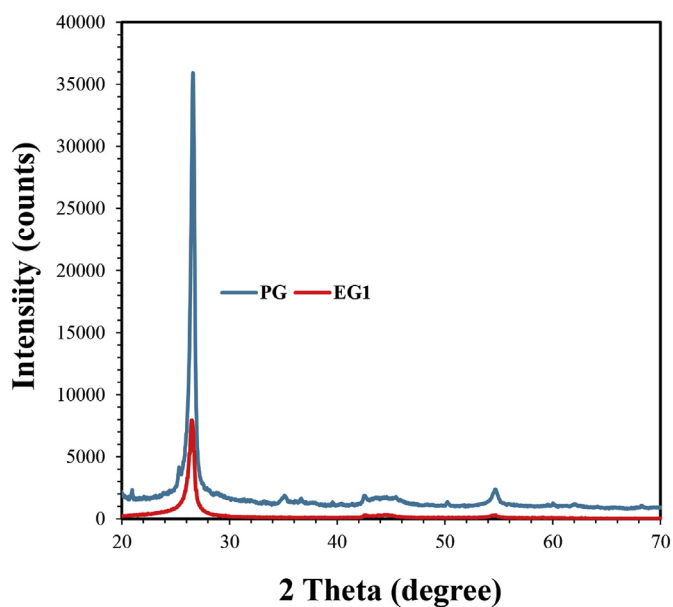


Fig. 2. XRD patterns of PG and EG1 samples.

2. Experimental

In this research, graphite electrodes, purchased from SGL group, were used as both anode and cathode. Sulfuric acid (H₂SO₄), sodium hydroxide (NaOH), hydrogen peroxide (H₂O₂) and distilled water were the materials used for preparing the electrolytes. Electrochemical

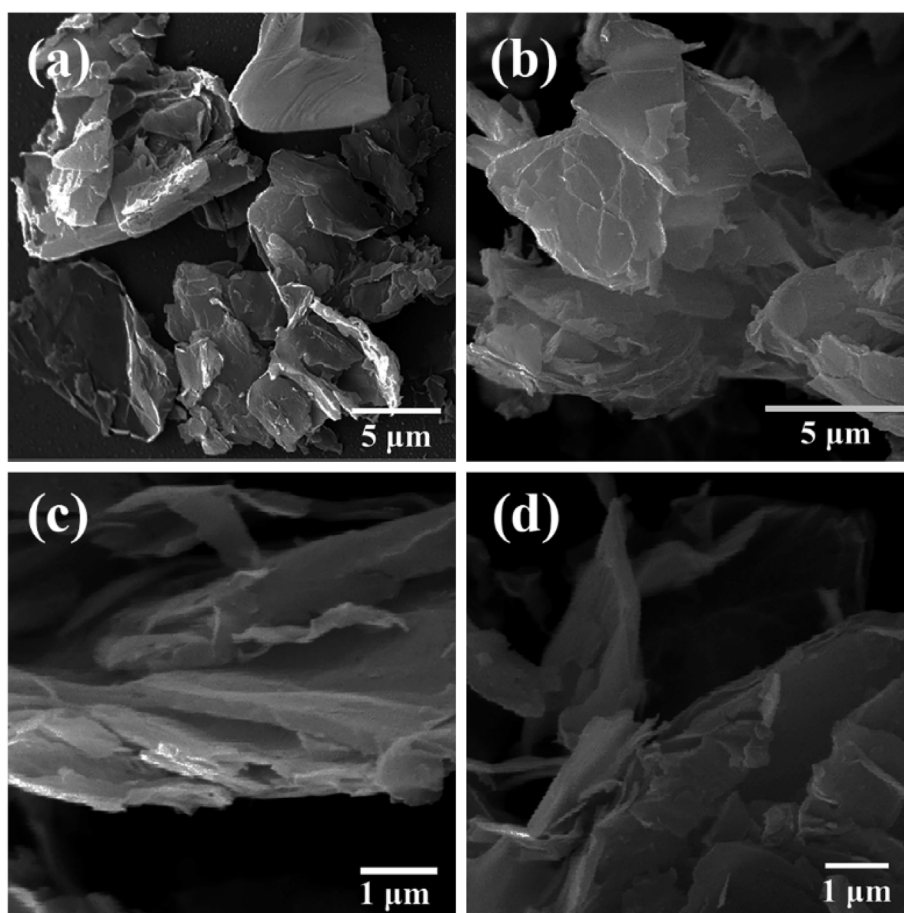


Fig. 1. SEM images of EG1 sample.

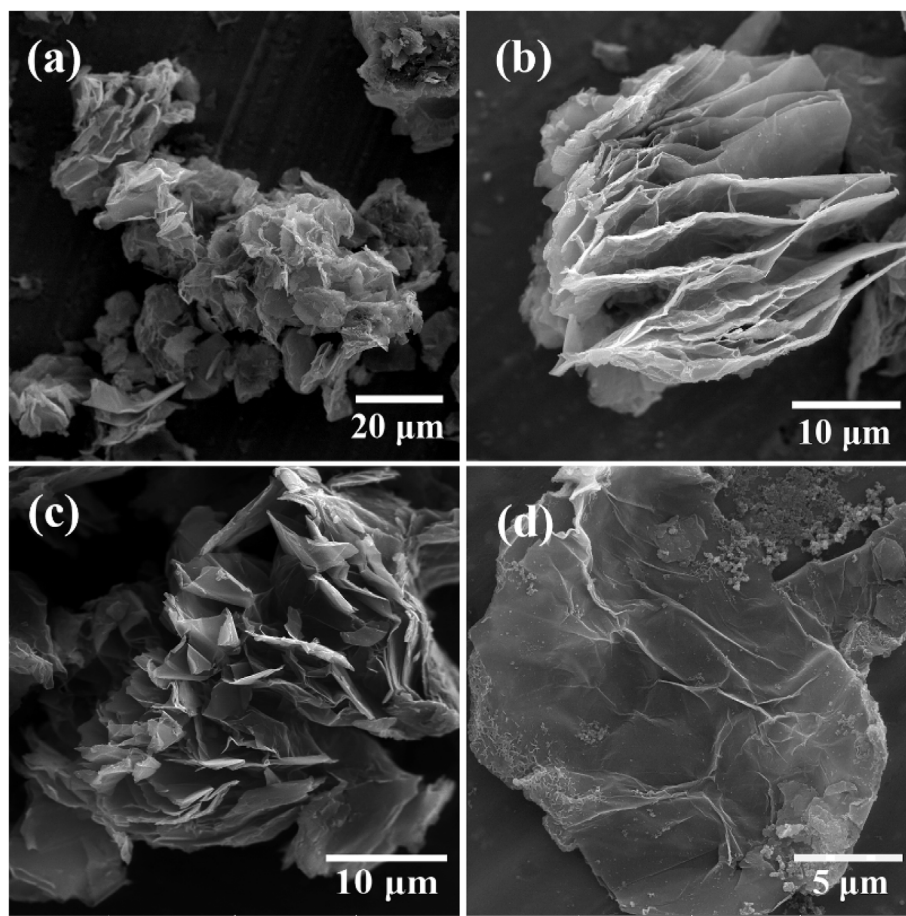


Fig. 3. SEM images of EG2 sample.

exfoliation was done using a DC power supply of 10 V. After that, the obtained exfoliated suspension was sonicated using a probe of 14 mm tip diameter, at 100 W for 15 min (ultrasonic homogenizer 400 W, 24 kHz, FAPAN Co., Iran). After sonication, the suspension was washed and filtered for three times with distilled water to remove impurities. Finally, the resulting material was dried by heating in a vacuum oven for 60 min at 100 °C to obtain exfoliated graphite (EG). The samples were codenamed as EG1, EG2, etc., as shown in Table 1.

Morphological evaluation of the obtained EG samples was performed by scanning SEM. XRD patterns were used for the phase analysis of the EG samples. The XRD analysis was performed using Cu K α radiation and a step scan of 0.05° for the 2 θ range of 20° - 70°. Transmission electron microscopy (TEM) images were taken using the FEI Tecnai F20 microscope. To characterize the defect density and number of layers in the EG samples, Raman spectroscopy analysis was used. Moreover, the FTIR spectrum was obtained by MOD SRG 1100G (Canada, BOMEM) spectrometer.

SAXS and WAXS experiments were conducted in the BL11-NCD beam-line at the ALBA Synchrotron light source facility, Spain. The beam spot size at the sample was 25 μm \times 25 μm and the wavelength of the monochromatic X-ray was 1.24 Å. Simultaneous SAXS/WAXS patterns of GNPs were recorded at room temperature with a sample to detector distance of 7573 mm and q range was set at min = 0.1933 Å⁻¹ and max = 6.030 Å⁻¹ with beam stop at 4 mm. The optimum powder sample was placed on polyimide adhesive tape. The intensity of the SAXS normalized as scattering cross section per unit volume of sample, $I(q)$, was generated by 10 keV of X-ray energy which is presented as a function of the scattering vector (q) defined as [18]:

$$q = 4\pi \frac{\sin(\theta)}{\lambda} \quad (1)$$

where θ is scattering angle or beam direction and λ is the wavelength of X-rays. The collected results were analyzed by using the SASfit software.

3. Results and discussion

In the first attempt of the experiments, a 1.6 M H₂SO₄ solution was chosen as the electrolyte. Fig. 1 shows SEM images of the EG1 obtained by electrochemical exfoliation in 1.6 M H₂SO₄ solution. The high thickness of resulted powders is visible in Fig. 1. From Fig. 1c and d, it can be deduced that a weak exfoliation process has occurred for graphite anode, demonstrating the low efficiency of 1.6 M H₂SO₄ in producing GNPs. Fig. 2 compares the XRD patterns of PG and EG1 samples. In both samples, the specific peak of graphite at about 26° is visible; the peak intensity of the EG1 is lower than that of PG sample, the intensity ratio of the EG1 to the PG is 0.221. The lower intensity of this peak reveals a lower crystallinity of graphite. Based on the SEM images of Fig. 1, it can be found that, although the electrochemical treatment caused lower peak intensity of the graphite, the exfoliation process did not take place adequately and so, the GNPs were obtained. During the experiment, it has been observed that graphite layers quickly drowned to the bottom of the container. Therefore, it could be expressed that, the efficiency of electrochemical exfoliation of graphite is significantly affected by the reaction kinetics. If kinetics of the process is fast, the intercalation and subsequently, exfoliation of graphite layers would not occur completely. Although H₂SO₄ is an effective electrolyte for exfoliation of graphite, using it as an electrolyte leads to fast electrochemical process. Accordingly, the kinetics of the process should be lowered.

Addition of an alkaline agent such as KOH, NaOH, etc. is a proper

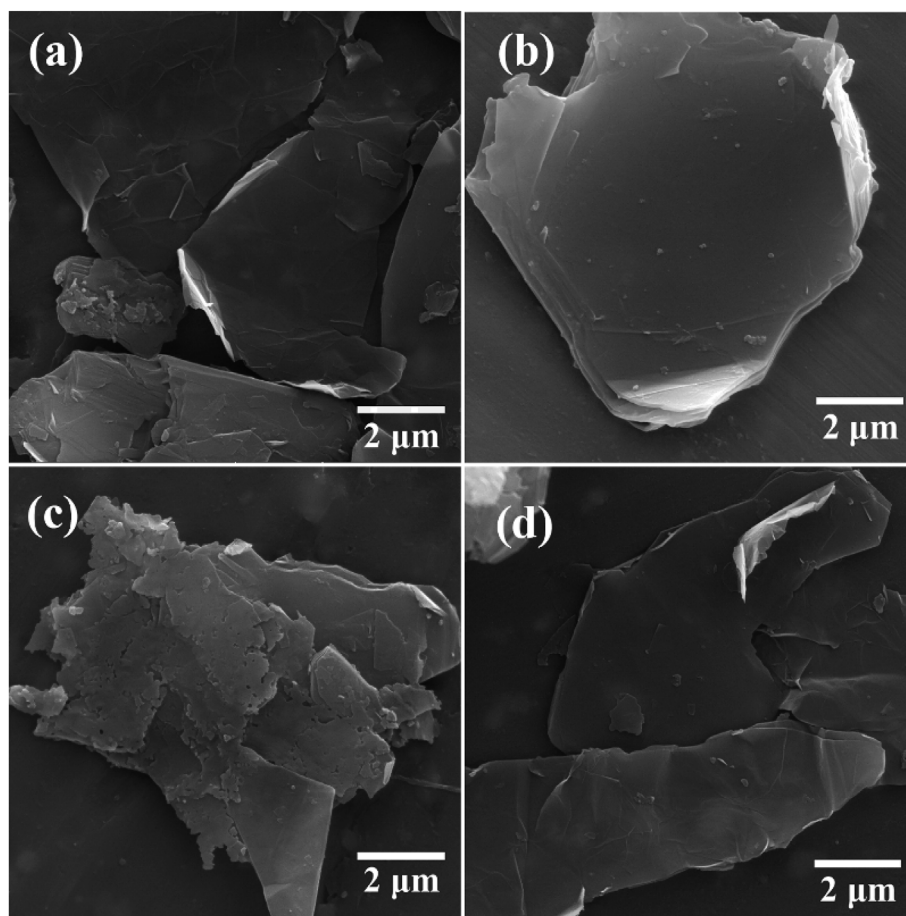


Fig. 4. SEM images of EG3 sample.

way for decreasing the kinetics of the process. In the literature, there are some works regarding the positive effects of H_2O_2 for improving the efficiency of electrochemical production of GNPs. For example, Rao et al. [19] successfully introduced a novel electrochemical method for GNPs production. They used $\text{NaOH}/\text{H}_2\text{O}_2/\text{H}_2\text{O}$ as the electrolyte and reported that the concentration of H_2O_2 had a great influence on the quality of the obtained GNPs; with increasing the content of H_2O_2 from 0 to 130 mM, the exfoliation degree of graphite significantly was increased. In the another study, Shaikh et al. [20] investigated the effects of temperature and different contents of H_2O_2 on the efficiency of electrochemical exfoliation of GNPs. The positive effects of H_2O_2 on the production of GNPs via electrochemical method were demonstrated in their study. Therefore, we used different mixtures of $\text{H}_2\text{SO}_4 + \text{NaOH} + \text{H}_2\text{O}_2$ as the electrolyte. In the second attempt of our experiments; three concentrations of 0.6, 1.2 and 1.6 M for H_2SO_4 were used while the concentrations of NaOH (0.03 M) and H_2O_2 (0.5 M) were kept constant.

Figs. 3–5 show the SEM images of obtained EG powders from electrolytes with different H_2SO_4 concentrations of 1.6, 1.2 and, 0.6 M, respectively. Fig. 3 shows the obtained powders from electrolyte with 1.6 M H_2SO_4 (EG2 sample). It is clear that a remarkable change has occurred with the addition of $\text{NaOH} + \text{H}_2\text{O}_2$ to the electrolyte. Visibly, the exfoliation process has been significantly improved in this condition. In other words, as visible in Fig. 3d, the transformation of graphite to GNPs has partially occurred in EG2 sample. Thereby, it can be said that a mixture of expanded graphite and graphene has been obtained after the addition of $\text{NaOH} + \text{H}_2\text{O}_2$ to the electrolyte.

Compared to the first attempt in this study, the improved electrochemical exfoliation of graphite can be attributed to two reasons. It seems that the addition of NaOH has reduced the kinetics of the process,

and the addition of H_2O_2 has played a significant role in improving the efficiency of the process. The produced hydroxyl ions by water decomposition caused opening the edges of graphite layers and consequently, led to enhancing the exfoliation process. However, the hydroxyl ions have low penetration ability and cannot effectively react with graphite. When H_2O_2 is added to the electrolyte, the reaction between H_2O_2 and hydroxyl ions results in producing O_2^{2-} and water. The presence of O_2^{2-} ions can effectively enhance the opening of the graphite layers.

Fig. 4 illustrates the SEM images of the obtained EG powders with the electrolyte containing 1.2 M H_2SO_4 (EG3 sample). As visible, a larger proportion of GNPs has been obtained using the 1.2 M H_2SO_4 , compared to the EG2 sample. In other words, the number of graphene layers in the EG3 sample is lower than that of the EG2 sample (Fig. 4b and c). The SEM images of EG powders with the electrolyte containing 0.6 M H_2SO_4 (EG4 sample) are shown in Fig. 5. It is quite evident that the graphene sheets are few-layered with high surface area, demonstrating the significant improvement in the exfoliation process of the graphite electrode. According to the SEM images, it can be deduced that with decreasing the concentrations of H_2SO_4 from 1.6 to 0.6 M, the efficiency of electrochemical exfoliation of graphite into GNPs has been found an improving trend.

The XRD patterns of PG, EG2, EG3 and EG4 samples are shown in Fig. 6. It is obvious that the main peak in the XRD pattern of the samples is around 26° . It is worth noting that the concentration of H_2SO_4 has played a significant role in the intensity of this peak; the lower concentration of H_2SO_4 is used, the lower peak intensity has resulted. The intensity ratio of EG4 to PG at 26° is about 0.067. This ratio is about three times smaller than that of EG1 sample. These observations clearly show the better exfoliation process in the mixture of

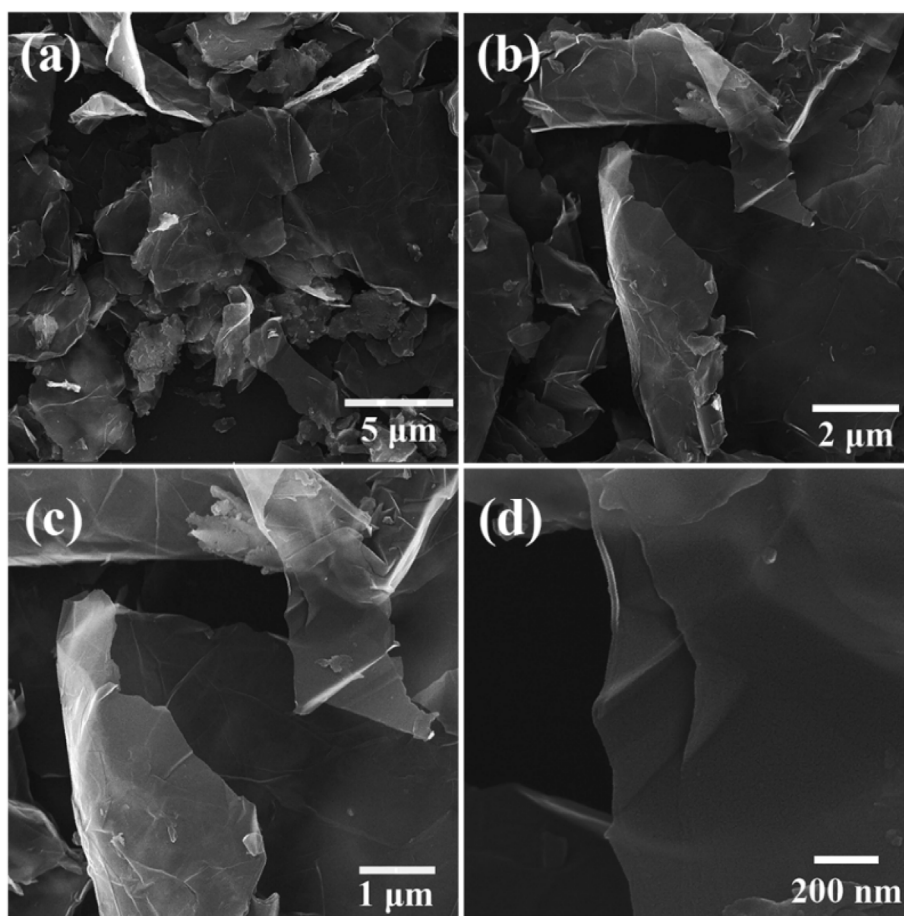


Fig. 5. SEM images of EG4 sample.

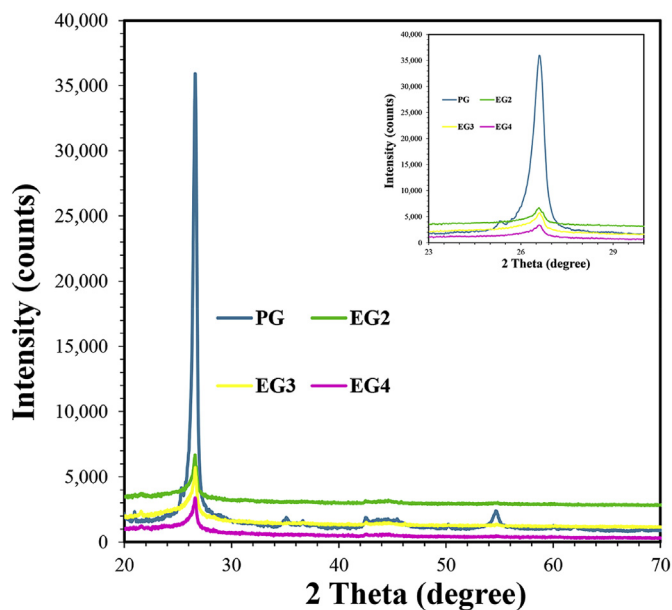


Fig. 6. XRD patterns of PG, EG2, EG3 and EG4 samples.

$\text{H}_2\text{SO}_4 + \text{NaOH} + \text{H}_2\text{O}_2$. In a similar study, Abdelkader et al. [21] showed that the diffraction peak at about 26.6° of the electrochemically exfoliated graphene has a lower intensity, compared to the graphite. This indicates that the graphite layers have been separated successfully. In the Singh et al. [22] study, the XRD peak intensity ratio of the graphene to graphite at $2\theta = 26^\circ$ was about 0.07.

Thereby, it can be said that the obtained GNPs in the electrolyte containing $0.6 \text{ M H}_2\text{SO}_4$ (EG4 sample) is the optimum sample, in our experiments. Therefore, the TEM images, Raman spectroscopy and FTIR analyses were performed for the EG4 sample. TEM images provide valuable information about the morphology and number of layers of graphene. Fig. 7 shows the TEM images of GNPs from EG4 sample. Different transparent regions are visible, showing the presence of GNPs with a different number of layers. Obviously, the darker zones reveal the presence of multi-layered GNPs while the brighter zones demonstrate the presence of few-layered GNPs.

Raman spectroscopy for EG4 sample is shown in Fig. 8. Raman spectroscopy is a useful and sensitive technique for determining defects and the number of layers of graphene. As shown, there are three peaks in the range of $1200\text{--}3000 \text{ cm}^{-1}$; 1338, 1569, and 2686 . These peaks, respectively, correspond to the D, G and 2D bands. The D peak indicates the presence of defects in the graphene structure. In addition, the G band is related to the sp^2 hybrid carbon atoms. The ratio $I_{\text{D}}/I_{\text{G}}$ represents the defect density of the GNPs. For example, in EG4 sample, the $I_{\text{D}}/I_{\text{G}}$ ratio is about 0.64, indicating a very low percentage of defects. The $I_{2\text{D}}/I_{\text{G}}$ ratio is another factor in determining the quality of graphene sheets. Higher $I_{2\text{D}}/I_{\text{G}}$ ratio indicates smaller number of layers. For single and bi-layer graphene sheets, the $I_{2\text{D}}/I_{\text{G}}$ ratio is 2 and 1, respectively. The 2D band at 2686 cm^{-1} and the intensity ratio, $I_{2\text{D}}/I_{\text{G}} = 0.719$, confirmed that although the GNPs in EG4 sample are not single or bi-layered, the number of graphene layers in this sample is low.

Tian et al. [11] used electrochemical route to produce high-quality with low oxygen content graphene as a simple and green method. It has been mentioned that in the acidic pH, the generation of O_2 from H_2O_2 would not react with graphite, and would release a large amount of CO_2

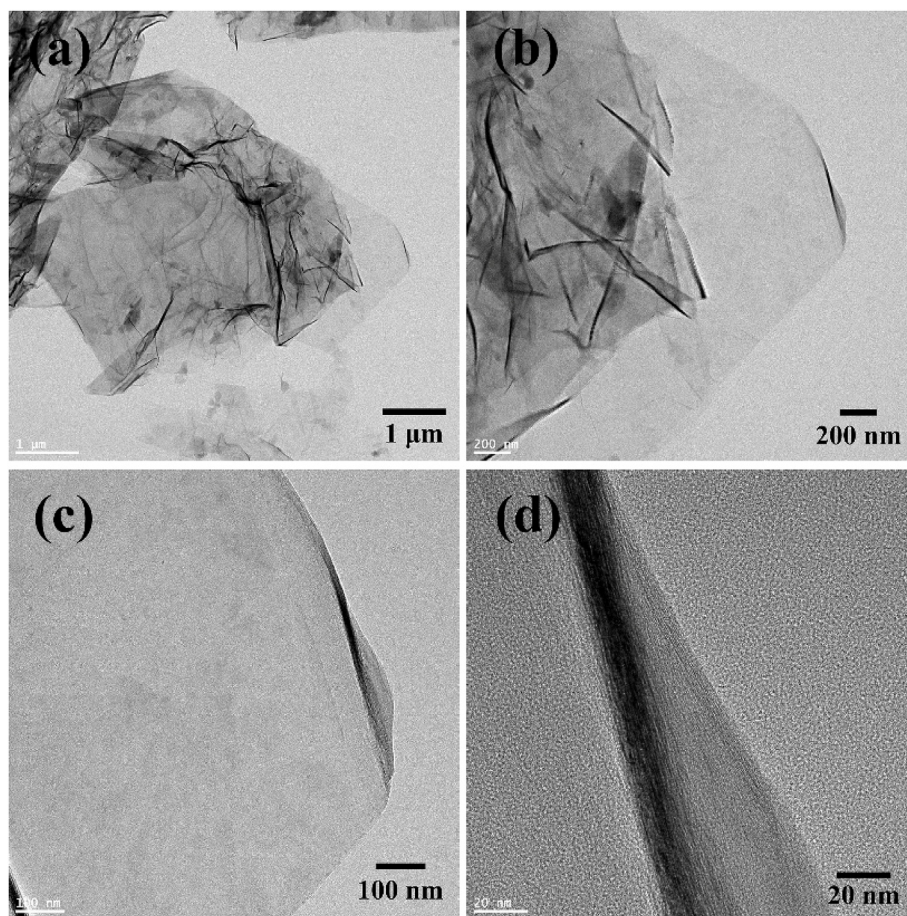


Fig. 7. TEM images of EG4 sample.

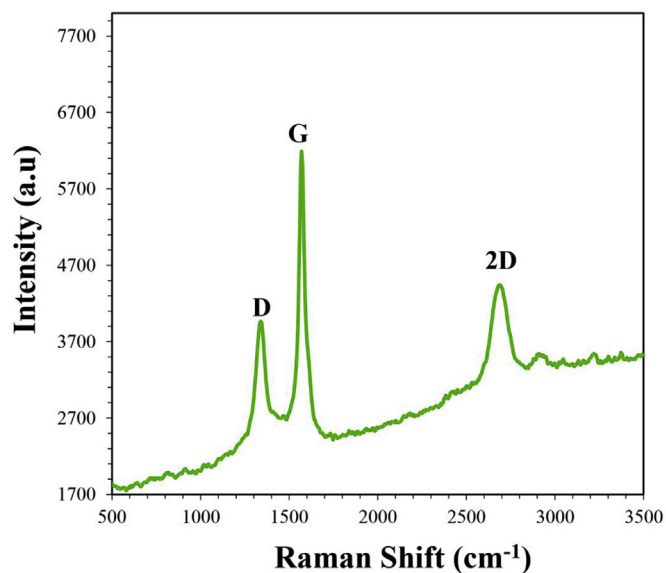


Fig. 8. Raman spectroscopy of EG4 sample.

gas to help exfoliation. The Raman spectrum of this study showed that the I_{2D}/I_G ratio is about 0.34. This value is much lower than that of our results, indicating the production of few-layered GNPs in our work. Singh et al. [22] reported that, in Raman spectroscopy analysis, the I_D/I_G and I_{2D}/I_G ratio of was respectively about 0.75 and 0.13 for graphite and 0.34 and 0.32 for graphene. Their Raman spectroscopy results for graphene showed the increase in the structural order and low number

of layers in graphene. Comparison between this study and our work clearly shows the lower number of layers in our obtained graphene.

Similarly, Gee et al. [16] produced graphene using electrochemical exfoliation of graphite in H_2SO_4 solution. In their work, the obtained I_D/I_G ratio (1.21) is so higher than that of our research, suggesting that graphene surface was partially oxidized because of H_2SO_4 intercalation. It has been reported that the I_{2D}/I_G ratio was about 0.36 and this value is much lower than that of our result, which the larger ratio represents the higher degree of sp^2 -hybridized carbon-carbon bonding in graphene structure.

Fig. 9 shows the FTIR spectroscopy analysis for the EG4 sample. Each peak reveals the presence of specific functional groups or bonds in the GNPs. It is important to note that the FTIR spectroscopy is a qualitative analysis for determining bonds. The presence of C–O bonds demonstrates the occurrence of the oxidation process of graphene sheets. Based on the acidic environment of electrolyte, the presence of C–O bonds is an expected phenomenon. The presence of OH, C–H, C=C and C–O groups confirm the basal and edge plane defects of GNPs and these defects are attributed to the electrochemical method used in producing them.

According to the above-mentioned results, it can be said that the efficiency of electrochemical exfoliation of graphite greatly depends on the type of electrolyte used; thick graphite plates, multi-layered GNPs and few-layered GNPs can be obtained based on electrolyte concentration. The mixture of $H_2SO_4 + NaOH + H_2O_2$ as electrolyte resulted in the production of high-quality and few-layered GNPs.

Typical SAXS results were extracted by collecting data from different locations on the adhesive tape because the graphene powder was not distributed uniformly on it. Data reduction was carried out to find the best results and the calculations were conducted to determine the

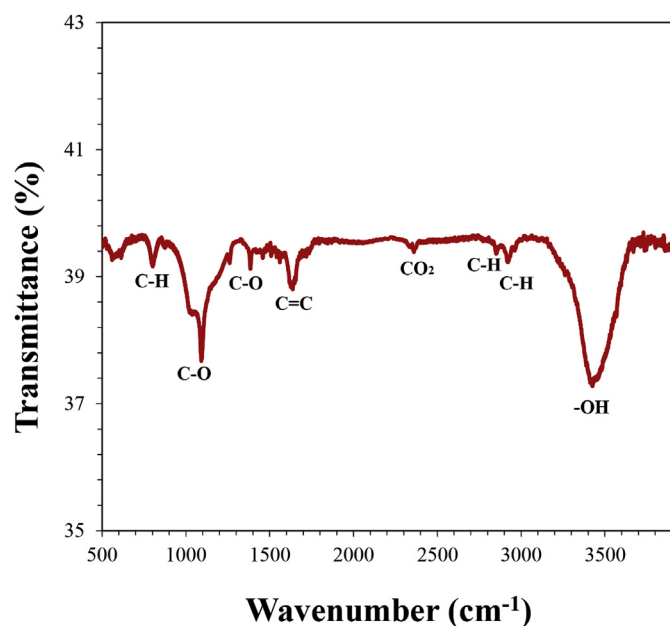


Fig. 9. FTIR Spectrum of EG4 sample.

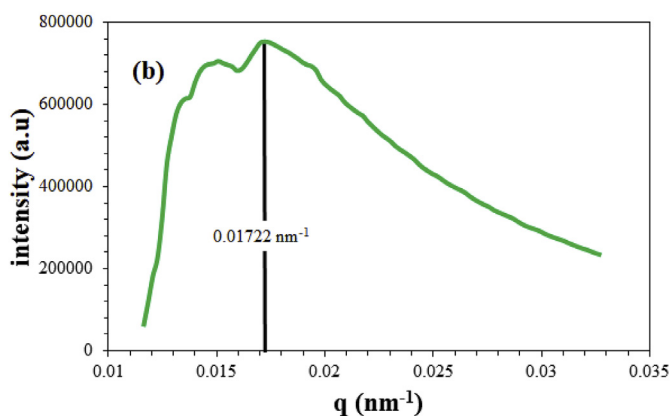
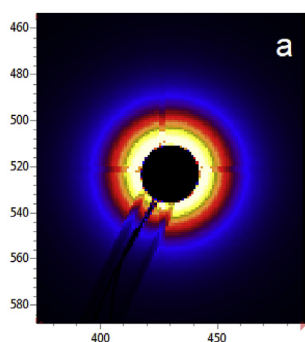


Fig. 10. Typical SAXS patterns with the respective radial profiles, a) 2D SAXS diffraction pattern of powder graphene sample (EG4), b) Radial profile of SAXS scattering corresponded to the irregular structure, a very low q ($q \sim 0.0172 \text{ \AA}^{-1}$) revealing mesoporous structure due to the exfoliated platelets.

parameters. The shown scattering pattern in Fig. 10a indicates crystalline structure with random layer, but this pattern does not necessarily present a specific feature so further integration and background correction are needed. In Fig. 10b, the space between nano-objects can be investigated from SAXS patterns by the radial profile after azimuthal integration. The interlayer spacing (d) can be calculated from the following equation (Eqn. (2)) [23]:

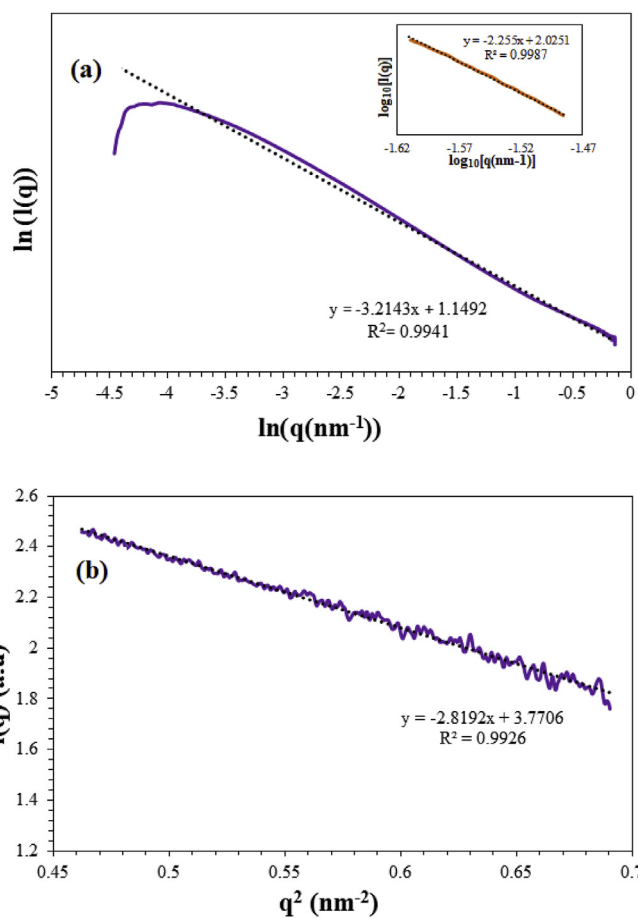


Fig. 11. a) SAXS fractional Porod's slope attributed to flake-like graphene of EG4, b) Linear fit to $y = a + bx$ to $\ln(Iq) = -(q^2) \cdot Rg^2/3 + \ln(I_0)$ for radius of gyration (Rg).

$$d = \frac{2\pi}{q} \quad (2)$$

where q is the scattering vector. The interlayer spacing for the exfoliated graphene nanoplatelets by the electrochemical process is about 36.5 nm which is much more than graphite interlayer space. It can be expressed that exfoliated layers may be stacked on each other onto the adhesive tape without any interlayer bonding.

Fractal means that a non-regular object possessing self-similarity on all scales. SAXS scattering in fractals follows a power law as $I(q) \sim q^{-\alpha} \rightarrow \ln(I(q)) \sim -\alpha \ln(q)$ where α is the slope of the linear part of the curve in the diagram of scattering intensity $I(q)$ versus scattering vector q . Therefore, it can be provided some parameters such as shape and size distribution with α value [24]. Different values of α correspond to different shapes; 1 for rods, 2 for discs and 3 for spheres. In some intermediate cases when $2 < \alpha < 3$, the objects possess a fractal geometry [23]. Accordingly, for the EG4 sample, the calculated value for α by fractional Porod's slope is 2.25 (Fig. 11a). This value for α implies the flake-like structure with a fractally rough surface of EG4 sample, indicating the aggregation of some particles. In other words, the calculated value for α can be attributed to the improper dispersion and distribution of GNPs.

The lower values of the scattering vector reveal that the size range of the particle is too big which has been measured using SAXS [25]. At the higher values of q , the change in curvature has been slightly appeared owing to the aggregation of small platelets or stacked on the big particles [26]. The bigger size of GNPs can be related to the exfoliation process by electrochemical or sonication processes. In other words, it can be deduced that these processes have not imposed enough energy to

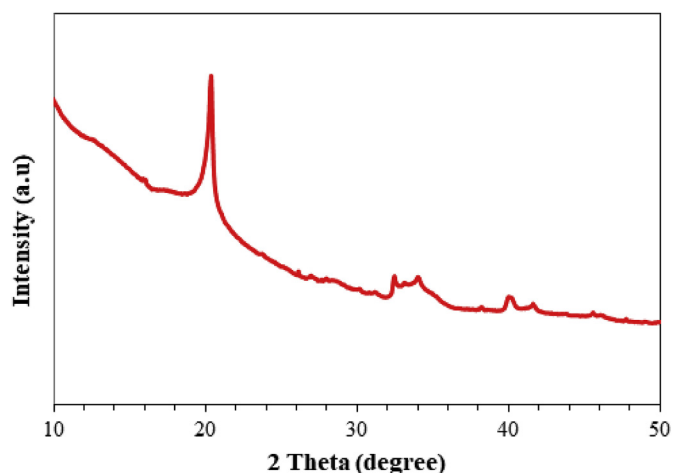


Fig. 12. WAXS pattern disclosing of crystalline domain attributed to GNPs of EG4 sample.

intercalation of the ions between the graphite layers [25]. The average grain radius R can be calculated from the radius of gyration (R_g) by estimating the slope in the linear fit of $\log(I)$ vs. $f(q)$. From this fit line (Fig. 11b), the shapes of disk was obtained as $2.6 \text{ nm} < R_g < 2.95 \text{ nm}$ using $\ln(I_q) = -(q^2) * R_g^2/3 + \ln(I_0)$. Nugraheni et al. [27] have investigated the structural feature of synthesized reduced graphene oxide (rGO) by SAXS scattering. They reported that the average fitting slope for powder rGO is 3.24, revealing a three-dimensional structure with a fractionally rough surface of rGO.

Fig. 12 shows a typical WAXS pattern with the same peaks attributed to the same phase in the sample of exfoliated graphene. In the graphene, the (002) and (100) planes are two main peaks as investigated in the patterns [28]. Due to the difference between the wavelength values, lattice parameter and interlayer spacing in WAXS and XRD methods, a peak shifting can be seen in Fig. 12, compared to the XRD patterns. The highly asymmetrical (002) peak is dealing with less accurate calculation number of graphene layers that can be attributed to the random arrangement and highly stacked graphene layers. A shift that occurs at the angle of $2\theta \sim 21^\circ$ is due to a difference in wavelength between WAXS of $\lambda = 1.24 \text{ \AA}$ and XRD of $\lambda = 1.54 \text{ \AA}$ (Cu-K α). In the top to down methods, the exfoliation method has been recognized as an important parameter on the number of layers, shape and broadness of (002) peak in the scattering pattern of graphene. In a study, the WAXS pattern of rGO showed a similar pattern to XRD data. The (002) peak was located at $2\theta = 23^\circ$, which a shift at the angle was due to the difference in wavelength between WAXS and XRD and the broadness of peak correspond to an amorphous structure that possibly was due to a pile of random arrangement of thick parallel layers [29].

4. Conclusions

In this study, the morphological evaluation of obtained powders after electrochemical exfoliation of graphite anode in the electrolytes containing H_2SO_4 was studied and the following results were drowned:

- 1 The efficiency of electrochemical exfoliation of graphite was significantly improved using the mixture of $\text{H}_2\text{SO}_4 + \text{NaOH} + \text{H}_2\text{O}_2$, compared to the H_2SO_4 electrolyte. Generally, the kinetics of the electrochemical process was controlled by the addition of NaOH and the expansion degree of layers was enhanced owing to the presences of H_2O_2 .
- 2 SEM observations clearly showed that with decreasing the concentration of H_2SO_4 from 1.6 to 0.6 M, the efficiency of the process was significantly improved; the lowest used concentration of H_2SO_4 resulted in the getting the few-layered graphene nanoplatelets. In

addition, the XRD peak intensity of powders had found a decreasing trend at 26° , showing the improvement in the exfoliation process of graphite.

- 3 Raman spectroscopy indicated that the I_D/I_G and I_{2D}/I_G ratio of the optimum sample was respectively about 0.64 and 0.719, confirming the low defect density and few layers of obtained graphene.
- 4 The SAXS results indicated the fractal of the surface as rough and disc shape with an interlayer spacing attributed to the exfoliation led to platelets with few layers of graphene plane. The SAXS results was in accordance with the previous results in TEM or Raman. The WAXS peak for the sample was shifted relatively to the XRD pattern, indicating a major peak belong to the exfoliated graphene nanoplatelets.

Acknowledgment

The authors would like to appreciate Armina Engineering Company-ARMINANO and Institute for Research in Fundamental Sciences (IPM)-Iranian light source facility for funding this project. Thanks to all colleagues in ALBA Synchrotron-Barcelona especially the kind staffs in NCD beamline.

References

- [1] J.H. Warner, F. Schaffel, M. Rummeli, A. Bachmatiuk, Graphene: Fundamentals and Emergent Applications: Newnes, (2012).
- [2] S. Eglar, Graphene. An introduction to the fundamentals and industrial applications edited by madhuri sharon and maheshwar sharon, *Angew. Chem. Int. Ed.* 55 (2016) 5122.
- [3] A.T. Najafabadi, E. Gyenge, High-yield graphene production by electrochemical exfoliation of graphite: novel ionic liquid (IL)-acetonitrile electrolyte with low IL content, *Carbon* 71 (2014) 58–69.
- [4] R. Al-Gaashani, A. Najjar, Y. Zakaria, S. Mansour, M.A. Atieh, XPS and structural studies of high quality graphene oxide and reduced graphene oxide prepared by different chemical oxidation methods, *Ceram. Int.* 45 (2019) 14439–14448.
- [5] C. Zhang, W. Lv, X. Xie, D. Tang, C. Liu, Q.-H. Yang, Towards low temperature thermal exfoliation of graphite oxide for graphene production, *Carbon* 62 (2013) 11–24.
- [6] M.A. Saiful Badri, M.M. Salleh, Md Noor Nfa, M.Y.A. Rahman, A.A. Umar, Green synthesis of few-layered graphene from aqueous processed graphite exfoliation for graphene thin film preparation, *Mater. Chem. Phys.* 193 (2017) 212–219.
- [7] H. Ma, Z. Shen, M. Yi, S. Ben, S. Liang, L. Liu, et al., Direct exfoliation of graphite in water with addition of ammonia solution, *J. Colloid Interface Sci.* 503 (2017) 68–75.
- [8] N. Lu, G. He, J. Liu, G. Liu, J. Li, Combustion synthesis of graphene for water treatment, *Ceram. Int.* 44 (2018) 2463–2469.
- [9] M. Jin, H.-K. Jeong, T.-H. Kim, K.P. So, Y. Cui, W.J. Yu, et al., Synthesis and systematic characterization of functionalized graphene sheets generated by thermal exfoliation at low temperature, *J. Phys. D Appl. Phys.* 43 (2010) 275402.
- [10] S. Bose, T. Kuila, N.H. Kim, J.H. Lee, Graphene Produced by Electrochemical Exfoliation, (2014), pp. 81–98.
- [11] S. Tian, P. He, L. Chen, H. Wang, G. Ding, X. Xie, Electrochemical fabrication of high quality graphene in mixed electrolyte for ultrafast electrothermal heater, *Chem. Mater.* 29 (2017) 6214–6219.
- [12] P. Yu, S.E. Lowe, G.P. Simon, Y.L. Zhong, Electrochemical exfoliation of graphite and production of functional graphene, *Curr. Opin. Colloid Interface Sci.* 20 (2015) 329–338.
- [13] M. Zhou, J. Tang, Q. Cheng, G. Xu, P. Cui, L.-C. Qin, Few-layer graphene obtained by electrochemical exfoliation of graphite cathode, *Chem. Phys. Lett.* 572 (2013) 61–65.
- [14] K. Parvez, Z.-S. Wu, R. Li, X. Liu, R. Graf, X. Feng, et al., Exfoliation of graphite into graphene in aqueous solutions of inorganic salts, *J. Am. Chem. Soc.* 136 (2014) 6083–6091.
- [15] J. Liu, C.K. Poh, D. Zhan, L. Lai, S.H. Lim, L. Wang, et al., Improved synthesis of graphene flakes from the multiple electrochemical exfoliation of graphite rod, *Nano Energy* 2 (2013) 377–386.
- [16] C.-M. Gee, C.-C. Tseng, F.-Y. Wu, H.-P. Chang, L.-J. Li, Y.-P. Hsieh, et al., Flexible transparent electrodes made of electrochemically exfoliated graphene sheets from low-cost graphite pieces, *Displays* 34 (2013) 315–319.
- [17] S. Aslam, F. Mustafa, M.A. Ahmad, Facile synthesis of graphene oxide with significant enhanced properties for optoelectronic and energy devices, *Ceram. Int.* 44 (2018) 6823–6828.
- [18] A. Turković, P. Dubček, M. Rakić, M. Lončarić, B. Etlinger, S. Bernstorff, SAXS/DSC/WAXD study of TiO₂ nanoparticles and the effect of γ -radiation on nanopolymer electrolyte, *Vacuum* 86 (2012) 750–753.
- [19] K.S. Rao, J. Senthilnathan, Y.F. Liu, M. Yoshimura, Role of peroxide ions in formation of graphene nanosheets by electrochemical exfoliation of graphite, *Sci. Rep.* 4 (2014) 4237.

- [20] S.T. Hossain, R. Wang, Electrochemical exfoliation of graphite: effect of temperature and hydrogen peroxide addition, *Electrochim. Acta* 216 (2016) 253–260.
- [21] A.M. Abdelkader, I.A. Kinloch, R.A. Dryfe, Continuous electrochemical exfoliation of micrometer-sized graphene using synergistic ion intercalations and organic solvents, *ACS Appl. Mater. Interfaces* 6 (2014) 1632–1639.
- [22] V.V. Singh, G. Gupta, A. Batra, A.K. Nigam, M. Boopathi, P.K. Gutch, et al., Greener electrochemical synthesis of high quality graphene nanosheets directly from pencil and its SPR sensing application, *Adv. Funct. Mater.* 22 (2012) 2352–2362.
- [23] T.A. Ezquerro, M.C. García-Gutiérrez, J.J. Hernández, A. Nogales, D.R. Rueda, X-ray scattering applied to the analysis of carbon nanotubes, polymers and nanocomposites. *Dispersión de rayos X aplicado al análisis de nanotubos de carbono, polímeros y nanocompuestos*, (2007).
- [24] W.-D. Cheng, C.-H. Ren, X.-H. Gu, Z.-J. Wu, X.-Q. Xing, G. Mo, et al., Microstructural changes of graphene/PLA/PBC nanofibers by electrospinning during tensile tests, *Chin. Phys. Lett.* 34 (2017) 036101.
- [25] A.Y. Nugraheni, D.N. Jayanti, Kurniasari, S. Soontaranon, E.G. Rachman Putra, Darminto, Structural analysis on reduced graphene oxide prepared from old coconut shell by synchrotron X-ray scattering, *IOP Conf. Ser. Mater. Sci. Eng.* 196 (2017) 012007.
- [26] B. Andonovic, A. Ademi, A. Grozdanov, P. Paunović, A.T. Dimitrov, Enhanced model for determining the number of graphene layers and their distribution from X-ray diffraction data, *Beilstein J. Nanotechnol.* 6 (2015) 2113–2122.
- [27] A.Y. Nugraheni, D.N. Jayanti, S. Soontaranon, E.G.R. Putra, Structural Analysis on Reduced Graphene Oxide Prepared from Old Coconut Shell by Synchrotron X-Ray Scattering. *IOP Conference Series: Materials Science and Engineering*, IOP Publishing, 2017012007.
- [28] N. Liu, F. Luo, H. Wu, Y. Liu, C. Zhang, J. Chen, One-step ionic-liquid-assisted electrochemical synthesis of ionic-liquid-functionalized graphene sheets directly from graphite, *Adv. Funct. Mater.* 18 (2008) 1518–1525.
- [29] R.L. Rubim, M.A. Barros, T. Missègue, K. Bougis, L. Navailles, F. Nallet, Highly confined stacks of graphene oxide sheets in water, *Eur. Phys. J. J.* 41 (2018) 30.